

Simulation of alfalfa yield with AquaCrop

Dirk Raes^{a,*}, Elias Fereres^b, Margarita García Vila^c, Yannick Curnel^d, David Knoded^e, Sema Kale Çelik^f, Yusuf Ucar^f, Mevlüt Türk^g, Joost Wellens^h

^a KU Leuven University, Department of Earth and Environmental Sciences, Celestijnenlaan 200E – PostBox 02411, B-3001 Leuven, Belgium

^b IAS-CSIC and University of Cordoba, Spain

^c Instituto de Agricultura Sostenible, CSIC, Spain

^d Centre wallon de Recherches agronomiques (CRA-W), Belgium

^e Fourrages Mieux, Marche-en-Famenne, Belgium

^f Department of Agricultural Structures and Irrigation, Faculty of Agriculture, Isparta University of Applied Sciences, 32200 Isparta, Turkey

^g Department of Field Crops, Faculty of Agriculture, Isparta University of Applied Science, 32200 Isparta, Turkey

^h TERRA Teaching and Research Centre & SPHERES Research Unit, University of Liège, 5030 Gembloux, 6700 Arlon, Belgium

ARTICLE INFO

Handling Editor - B.E. Clothier

Keywords:

AquaCrop

Crop simulation models

Alfalfa

Perennial forage crops

Transfer of assimilates

Length of growing cycle

Natural self-thinning

ABSTRACT

The AquaCrop simulation model, originally designed for annual crops, is expanded here to simulate alfalfa, a perennial forage crop. A new routine was added to the model to mimic the assimilate partitioning between above and below-ground plant parts to account for the utilization of reserves in Spring and for their storage in the Fall. The simulation of the transfer of assimilates requires only three extra crop parameters which makes the model also easy to calibrate. To evaluate the model, yield data collected in Louvain-La-Neuve (Belgium), Isparta (Turkey), and Ottawa (Canada) for different alfalfa cultivars, various years and field and irrigation management strategies were used. To assess the accuracy and robustness of the simple assimilate remobilization process, simulations were run for the three different environments with a common set of crop parameters which were parameterized. The dispersion between the observed and simulated cumulative dry above-ground biomass during the growing cycle was small ($r^2 = 0.97$; nRMSE = 11%; Nash-Sutcliffe model EF = 0.97), and a systematic over- or underestimation by the model was not observed (Willmott's index of agreement, $d = 0.99$). When evaluating the goodness of fit of the 81 individual harvest events, the results were still very satisfactory although the nRMSE doubled. The simulations indicated that the AquaCrop model adapted to perennial crops and with a novel storage-remobilization routine, could predict well alfalfa yields in various climates and environments, with and without water and fertility stress, and for three different alfalfa cultivars.

1. Introduction

Alfalfa (*Medicago sativa* L.) is the world's leading forage crop, a perennial legume that has high nutritional value and a deep root system capable of extracting water and nutrients from the subsoil. Alfalfa is an ancient crop which originated in South-Central Asia and has spread rapidly to the Mediterranean Basin, and eventually to South and North America. Yuegao and Cash (2009) state that production takes place in a global area of about 30 million ha since the 1990 s: off which 41% in North America (mainly US and Canada), 25% in Europe, 23% in South America (mainly Argentina), 8% in Asia (mainly Russia and China), 2% in Africa and 1% in Oceania. Alfalfa is essential in the animal husbandry food chain being used as hay, silage, or pellets; and is as such worldwide

traded as a commodity (FAOSTAT, 2022). It can be produced under rainfed or irrigated conditions and is harvested or cut several times a year depending on climatic conditions and management. Harvest management has proven to significantly impact yields (Moot et al., 2003; Orloff and Putnam, 2007; Teixeira et al., 2008). Asseng and Hsiao (2000) have demonstrated that alfalfa water productivity is very high once the costs of symbiotic N fixation, higher protein content and different partitioning to below ground organs are accounted for.

Given the ever-higher pressure on agricultural land-use, changing diets characterised by a higher meat consumption and climate change induced uncertainties, crop growth models can be a straightforward and cost-effective tool to assess crop performance (Di Paola et al., 2015), yield gaps (Guilpart et al., 2017), and to assist in decision making at the

* Corresponding author.

E-mail address: dirk.raes@kuleuven.be (D. Raes).

<https://doi.org/10.1016/j.agwat.2023.108341>

Received 13 March 2023; Received in revised form 24 April 2023; Accepted 29 April 2023

Available online 3 May 2023

0378-3774/© 2023 Published by Elsevier B.V. This is an open access article under the CC BY-NC-ND license (<http://creativecommons.org/licenses/by-nc-nd/4.0/>).

operational, tactical and strategic levels (van Keulen and Asseng, 2019; Loomis and Connor, 2012). Models have also been used to improve current and future agricultural itineraries, and hence provide support for agricultural programmes or policies.

The initial crop simulation models focused on annual crops while modelling of crops such as perennial forage crops have lagged behind. Nevertheless, there have been attempts at either developing specific alfalfa models or adapting existing crop models to alfalfa. A review of existing alfalfa models has been presented by Malik et al. (2018). The DSSAT model (Hoogenboom et al., 2019) has adapted its integrated CSM-CROPGRO-PFM (Perennial Forage Model) to simulate alfalfa biomass production in Northeast Spain (Malik et al., 2018) and eastern Canada (Jing et al., 2020). The APSIM model (Keating et al., 2003) has been extensively tested for alfalfa in Australia and evaluated in the Argentine Pampas and south-eastern Australia (Ojeda et al., 2016) and China (Peng et al., 2022). In France, another major alfalfa producer, Strullu et al. (2020) obtained biomass regrowth estimates using the STICS model (Brisson et al., 1998). In Northern Italy, Confalonieri and Bechini (2004) calibrated CropSyst for 2 alfalfa meadows. Other widely used simulation models such as AquaCrop are not capable to simulate alfalfa at present (Raes et al., 2009).

The design of the AquaCrop model pursued an optimum balance between simplicity, accuracy, and robustness (Steduto et al., 2009; Raes et al., 2009; Steduto et al., 2012; Vanuytrecht et al., 2014). With a relatively small number of crop parameters, AquaCrop is capable of simulating the attainable yield of the major annual herbaceous crops (and a few less common) (Farahani et al., 2009; García-Vila et al., 2009; García-Vila et al., 2019; Geerts et al., 2009; Heng et al., 2009; Hsiao et al., 2009; Todorovic et al., 2009; Wellens et al., 2013; Kumar et al., 2014; Tsegay et al., 2015; Araya et al., 2016; Razzaghi et al., 2017; García-Vila et al., 2019; Salman et al., 2021).

Here we report the work aimed at simulating the productivity of alfalfa with AquaCrop by adapting Version 7 of the model to simulate perennial herbaceous forage crops (Raes et al., 2022). A simple routine describes the transfer of assimilates between the above ground biomass and the below-ground storage organs. In the paper it was assessed if AquaCrop could be adapted to simulate perennial herbaceous forage crops, and that the transfer of assimilates between the above ground biomass and the below-ground storage organs could be simulated with a novel subroutine. To test this hypothesis, the model was first parameterized and subsequently, all simulations were run with a common set of crop parameters for different years, alfalfa cultivars, climates, field and irrigation management strategies.

2. Material and methods

2.1. Field experimental data

Yield (biomass) data of all individual harvest events of different alfalfa growing seasons were collected in Louvain-La-Neuve (Belgium) and Isparta (Turkey). Yield data for Ottawa (Canada), which also contained several biomass sampling dates between harvests, was extracted from Jing et al. (2020). Tables 1 to 4 present the coordinates, climate, soil type, irrigation and soil fertility management, cultivars, and the observed yields (dry matter) for the three locations. In Chapters 1–3 of

Table 1
Coordinates of the three study sites.

Location	Country	Latitude	Longitude	Altitude
Louvain-La-Neuve (LLN)	Belgium	50° 40' 5.84" N	4° 36' 51.95" E	131 m.a.s.l.
Isparta	Turkey	37° 46' 4.81" N	30° 33' 42.86" E	1049 m.a.s.l.
Ottawa	Canada	45° 25' 29.00" N	75° 41' 42.00" W	70 m.a.s.l.

Table 2

Climate classification and average annual rainfall (Rain) and reference evapotranspiration (ET_o) for the years of cultivation in the 3 study sites.

Site	Köppen climate classification	Description	Rain mm	ET _o mm
LLN	Cfb: Marine West Coast Climate	Cool and humid summer, and relative mild and rainy winter	666	692
Isparta	Csa: Hot-summer Mediterranean	Hot and dry summer, and chilly, rainy and often snowy winter	497	1034
Ottawa	Dfb: Warm Summer Continental Climate	Warm, humid summer, and a very cold winter	900	621

Table 3

Soil type, Total Available soil Water (TAW), and irrigation and soil fertility management in the three study sites.

Location	Soil type	TAW	Irrigation strategy	Soil fertility
LLN	Loamy sand	80 mm/m	Rainfed	well fertilized
Isparta	Sandy clay	140 mm/m	0, 25, 50, 75, 100% ET irrigated	well fertilized
Ottawa	Sandy loam	160 mm/m	Rainfed	limited

the supplementary material, more detailed information is provided regarding the climatic data, physical soil properties for these three sites and the irrigation schedule.

2.2. AquaCrop simulation processes

2.2.1. AquaCrop general calculation scheme

The calculation approach of AquaCrop consists of the successive simulation of (i) the green canopy cover, (ii) crop transpiration, (iii) biomass production and (iv) crop yield, all for each day of the growing cycle, as previously described by Steduto et al. (2009) and Raes et al. (2009).

The green canopy cover (CC) is the fraction of the soil surface covered by the canopy. For non-limiting conditions, the increase of CC is described by a Canopy Growth Coefficient (CGC). Driven by temperature, CC increases from the canopy cover at germination (CC_o) to a maximum value (CC_x) which can reach 1 if full canopy cover is reached. Both CC_o and CC_x are influenced by plant density.

Crop transpiration (Tr_i) is proportional to the simulated CC_i at day i. By using a biomass water productivity factor (WP*), AquaCrop calculates the daily above-ground biomass (b_i) from daily transpiration normalized for climate (using the reference evapotranspiration, ET_{o,i}):

$$B = \sum b_i = WP^* \sum \left(\frac{Tr_i}{ET_{o,i}} \right) \quad (1)$$

where B is the total above ground biomass produced during the growing cycle, and WP* is normalized for climate and CO₂ concentration.

A fraction of the simulated seasonal above ground biomass (B), the harvest index (HI) is partitioned to the harvestable organs to give the yield. A single value of WP* is used for the entire crop cycle for most crops. However, in crops where the composition of the harvestable product is rich in oil and/or protein such as sunflower, soybean and cotton, the WP* is reduced during yield formation to account for the fact that more photosynthates are required per unit of dry matter (Steduto et al., 2009). A correction factor makes that the WP* for those crops is gradually reduced during yield formation. Note that the calculations described above are affected by the occurrence of temperature, water, soil fertility and salinity stresses as described in detail in Steduto et al.

Table 4

The Location, alfalfa cultivar, sowing date, number of harvests (Cuts) and dry matter yield (Y in t/ha) for the 3 study sites.

Location	Cultivar	Sowing	1 st year		2 nd year		3 rd year	
			Cuts	Y	Cuts	Y	Cuts	Y
LLN	Artemis	8/5/2013	5	22.9	4	17.3	4	21.2
Isparta (100% ET irr)	Bilensoy	1/5/2017	6	28.2	6	28.2a	-	-
Isparta (75% ET irr)	Bilensoy	1/5/2017	6	26.6	6	21.4a	-	-
Isparta (50% ET irr)	Bilensoy	1/5/2017	6	25.8	6	25.1a	-	-
Isparta (25% ET irr)	Bilensoy	1/5/2017	6	20.6	6	18.4a	-	-
Isparta (rainfed)	Bilensoy	1/5/2017	6	15.2	6	13.6a	-	-
Ottawa	Unknown	21/5/2014	3	10.9	3	10.3	-	-

^a Since the 1st and 2nd years in Isparta have very similar climatic data (air temperatures, ETo and GDD), some uncertainty in the data was assessed. To align the reported 2nd year alfalfa yield with that of the 1st year, the data from the 6 cuts and 5 treatments were uniformly reduced by 25%.

(2009) and in Raes et al. (2022).

2.2.2. Adjustments of the simulation processes for herbaceous forage crops

2.2.2.1. Transfer of assimilates between above and below-ground plant parts. Perennial herbaceous forage crops allocate the carbon assimilated through photosynthesis (b_i) to above (leaves and stems) and below-ground organs (crowns and roots). Since AquaCrop does not simulate biomass partitioning among various organs, variations in partitioning along the season was simulated by increasing or reducing WP^* , as it is done for the energy-rich yield products of some crops during yield formation (Steduto et al., 2009). The above-ground biomass (B_{upper}) is simulated as:

$$B_{upper} = \sum f_i b_i = f_i \cdot WP^* \cdot \sum \left(\frac{Tr_i}{ET_{O_i}} \right) \quad (2)$$

Where f_i is a correction factor which is less than one during the period of assimilate storage in below-ground organs, and greater than one during the period of remobilization of assimilates in spring. The net assimilate storage stage starts after mid-season when the crop transfers an important fraction of b_i to the below-ground organs. During the following spring, which corresponds to the net remobilization stage, the stored assimilates are transferred to the above-ground organs to contribute to enhanced growth (Fig. 1). In the remobilization and storage stages, f_i is corrected for regrowth, since plants use the carbohydrate reserves for regrowth both in the spring and after each cutting (Undersander et al., 2011).

2.2.2.2. Storage of assimilates below ground (storage stage). Since perennial herbaceous forage crops transfer a considerable fraction of the assimilates below ground after mid-season (Teixeira et al., 2008; Moot et al., 2012), the daily biomass produced, b_i , is reduced by a fraction ($f_{sto,i}$, Eq.3) that exponentially increases from 0 at the start of the net storage stage ($t = 0$) to a fraction (S) of b_i at the end of the season ($t = 1$):

$$f_{sto,i} = \left[\frac{(\exp^{-5t} - 1)}{(\exp^{-5} - 1)} \right] S \quad (3)$$

When the crop is harvested during the storage stage, $f_{sto,i}$ is temporarily reduced to consider the assimilates required for the regrowth of the crop canopy. This is simulated by multiplying $f_{sto,i}$ by another adjustment factor (a_i , Eq.4) for regrowth ($0 \leq a_i \leq 1$):

$$a_i = \frac{(CC_i - CC_{cut})}{(CC_x - CC_{cut})} \quad (4)$$

where CC_{cut} is the canopy cover after harvest, and CC_i the canopy cover at day i , which increases during regrowth from CC_{cut} to the maximum canopy cover, CC_x . At every harvest date, $CC_i = CC_{cut}$, a_i is zero and storage is halted (Fig. 1). When CC_i reaches CC_x at the end of regrowth, a_i is 1, and storage is again at maximum rate.

2.2.2.3. Remobilization of assimilates from below ground (remobilization stage). Not all assimilates can be recovered from storage (Avicé et al., 1996). In AquaCrop it is assumed that of the total assimilates stored below ground in the previous season ($B_{sto,(n-1)}$), a fraction (M) is remobilized during the next season ($B_{mob,n}$, Eq. 5). The rest is assumed to be

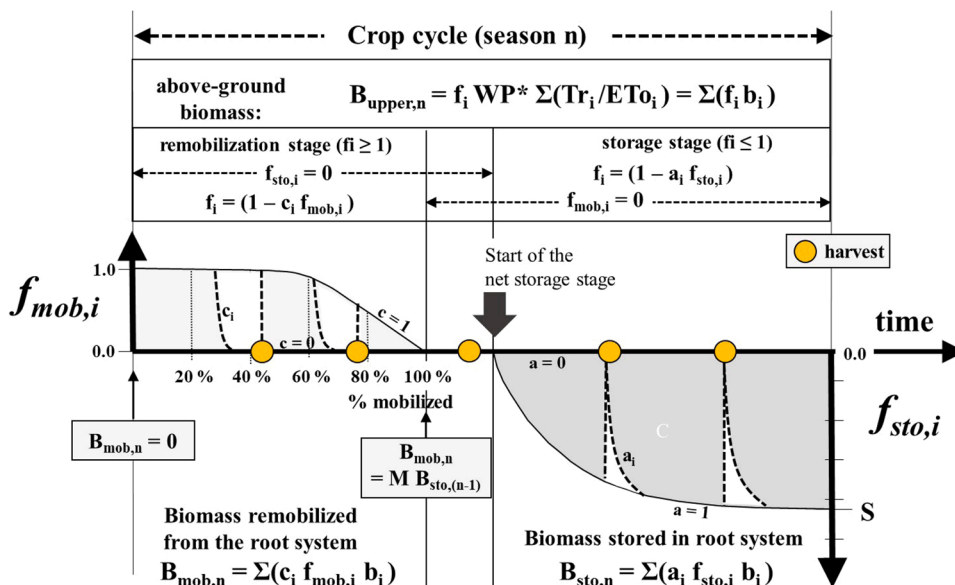


Fig. 1. Schematic representation of the simulation of the total above-ground biomass ($B_{upper,n}$) in the nth season, for alfalfa. During the spring (net remobilization stage), the transfer to the above-ground parts of the M th fraction of the assimilates stored below ground in the previous season ($B_{sto,(n-1)}$), is simulated by increasing the biomass at day i (b_i) with a fraction ($c_i f_{mob,i}$). To stimulate growth, the adjustment factor c_i is 1 as long as CC increase. When the maximum canopy cover is reached, c_i is zero and remobilisation is halted. From mid-season (start of the net storage stage), a fraction ($a_i f_{sto,i}$) of b_i is stored in the root system. The adjustment factor a_i for regrowth is zero on a day of harvest, and gradually increases to 1 during regrowth. For further explanation, see text.

lost by respiration and natural self-thinning, or to remain stored below ground:

$$B_{mob,n} = M - B_{sto,(n-1)} \quad (5)$$

Furthermore, it is assumed that at the start of the first year after sowing, only 20% of M is remobilized above ground, as many of the stored assimilates in the sowing year were required in the development and establishment of the perennial plant parts below ground (crown and root system).

To simulate the remobilization of stored assimilates at the start of the season, b_i is increased with a fraction ($f_{mob,i}$, Eq. 6) which decreases gradually as more and more assimilates are remobilized (Fig. 1):

$$f_{mob,i} = \frac{(\exp^{-5t} - 1)}{(\exp^{-5} - 1)} \quad (6)$$

$$t = \frac{B_{mob,n} - \sum b_{mob,i}}{B_{mob,n}} \quad (7)$$

where $b_{mob,i}$ are the assimilates remobilized from the root system on day i , expressed as a fraction ($f_{mob,i}$) of b_i , and t is the relative time in the remobilization stage which gradually decreases from 1 at the start of the season to zero at the end of the remobilization stage.

When the canopy reaches 90% of CCx after regrowth, remobilization is no longer considered. This is simulated by multiplying $f_{mob,i}$ with an adjustment factor (c_i) for regrowth ($0 \leq c_i \leq 1$):

$$c_i = \frac{(CC_x - CC_i)}{0.1CC_x} \text{ if } CC_i > 0.9CC_x \quad (8)$$

At each harvest, c_i is 1 and remobilization starts at its maximum rate. It stays that way until CC has reached 90% of its maximum (CCx). When maximum canopy cover is reached ($CC = CC_x$), c_i is zero and remobilization is halted until the next harvest. It is considered that remobilization and storage do not occur at the same time.

2.2.2.4. Length of the growing cycle. In AquaCrop, the length of the crop growing cycle is determined by the thermal regime of the season. For annual crops, crop maturity is reached when the sum of the daily growing degree days (GDD) since planting, reaches a predetermined value which is cultivar specific. As a result, the growing cycle will be longer in cold years and shorter in warm years. For perennial crops it is the opposite, the growing cycle will be shorter in cold years and longer in warm years. This is simulated by determining the start (for non-planting years) and end of the growing cycle by an air temperature criterion which is based either on the average air temperature or the sum of GDD over a number of days. By appraising the air temperature data, AquaCrop determines the restart and end of alfalfa growth within a specified time window at the beginning (onset) and end of the year. To avoid the generation of a restart in the early stages of spring when air temperatures might still drop sharply after an early start, AquaCrop offers the option to select the 2nd or 3rd occurrence of the selected criterion. Similarly, a 2nd or 3rd occurrence for the selected criterion in the late autumn or early winter can be selected, to avoid a premature ending of the growing period during a cold period before the final end of the season (Raes et al., 2022).

2.2.2.5. Natural self-thinning. The initial plant population of perennials progressively self-thins over the years. This is induced by climatic factors such as killing frosts, and by field management. The natural self-thinning results in a gradual decrease of CCx. Since initially the self-thinning is compensated by an increase in the number of shoots per plant to occupy the vacant space, the process does not decrease CCx in the first year but becomes only visible in later years when the plant population becomes smaller. The process of self-thinning can be calibrated in AquaCrop by considering the environment (climate) and field management (Raes et al., 2022). In a self-thinned plant population,

weed infestation might become important. A calculation process in AquaCrop allows the simulation of canopy development and crop production in weed-infested fields (Van Gaelen et al., 2016).

It would be desirable to test the effects of different self-thinning levels on the simulated yields. The limited number of successive years of the data used here for calibration does not allow to validate the simulation of natural self-thinning on yields.

2.3. Parametrization and Calibration

2.3.1. Crop parameters

To evaluate the accuracy and robustness of the simulation process of the transfer of assimilates, a common set of crop parameters was used (Table 5) to simulate production of different alfalfa cultivars in three

Table 5
Common set of AquaCrop crop parameters for alfalfa in the three study sites.

Crop parameter	Value	Source
A. Conservative and/or crop specific parameters		
■ Air temperature stress		
T_{base} : Base temperature (°C)	5	Lit
T_{upper} : Upper temperature (°C)	30	Est
Minimum growing degrees required for full crop transpiration (GDD.day ⁻¹)	8	Est
■ Soil water stress		
Soil water depletion for canopy expansion - Upper threshold (fraction of TAW)	0.15	Est
Soil water depletion for canopy expansion - Lower threshold (fraction of TAW)	0.55	Est
Shape factor for water stress coefficient for canopy expansion	3.0	Default
Soil water depletion for stomatal control - Upper threshold (fraction of TAW)	0.60	Est
Shape factor for water stress coefficient for stomatal control	3.0	Default
Soil water depletion for canopy senescence - Upper threshold (fraction of TAW)	0.70	Est
Shape factor for water stress coefficient for canopy senescence	3.0	Default
Soil water stress at which deficient aeration occurs (vol% below saturation)	5	Default
■ Soil salinity stress		
Electrical Conductivity of soil saturation extract at which crop starts to be affected by soil salinity (dS/m)	2	FAO29
Electrical Conductivity of soil saturation extract at which crop can no longer grow (dS/m)	16	FAO29
■ Development of Crop Canopy Cover		
Canopy growth coefficient (CGC) (increase of the fraction soil cover per growing degree)	0.012	Est
Canopy decline coefficient (CDC) (decrease of the fraction soil cover per growing degree)	0.006	Est
Soil surface covered by an individual seedling at 90% emergence (cm ²)	2.0	Est
■ Crop transpiration and biomass production		
K_{C-Trx} : Crop coefficient when canopy is complete but prior to senescence	1.15	Est
f_{age} : Decline of crop coefficient as a result of ageing, nitrogen deficiency, etc. (%/day)	0.050	Est
Water Productivity normalized for ET _o and CO ₂ (gram/m ²)	15.0	Cal
B. Non-conservatives and/or cultivar specific parameters		
Minimum effective rooting depth (m)	0.30	Default
Maximum effective rooting depth (m)	3.00	Lit
Shape factor describing root zone expansion	15	Default
Maximum root water extraction in top quarter of root zone (m ³ water/m ³ soil.day)	0.020	Default
Maximum root water extraction in bottom quarter of root zone (m ³ water/m ³ soil.day)	0.010	Default
Effect of canopy cover in reducing soil evaporation in late season stage	60	Default
Number of plants per hectare	2500,000	
Maximum canopy cover (CCx) in fraction soil cover	0.95	Est

Lit: literature; Est: estimation based on authors' experience with AquaCrop; FAO56: FAO Irrigation and Drainage paper N° 56 (Allen et al., 1998); FAO29: FAO Irrigation and Drainage Paper N° 29 (Ayers and Westcot, 1985); Default: AquaCrop default values.

different environments and years. Given the limited amount of observed data, indicative values for crop parameters were obtained from literature. In the absence of published data, values were estimated or default settings in AquaCrop were used. Parameter values in Table 5 need to be further tested in other environment and management conditions. Only the WP* was calibrated using a limited set of the observed yield data.

2.3.1.1. Air temperature stress. There is consensus that the T_{base} for alfalfa is 5 °C (Baral et al., 2022). A typical value for T_{upper} of calibrated crops in AquaCrop is 30 °C. It is the temperature above which crop development no longer increase with an increase in air temperature. Since it has only an effect when the average air temperature (required to calculate GDD) rises above T_{upper} , which never occurred in the study sites, T_{upper} could not be evaluated.

The minimum growing degrees required in a day for full crop transpiration, is typically an estimated crop parameter in AquaCrop since it is hard to obtain from field data. By considering calibrated crops with a similar low T_{base} , a minimum of 8 GDD per day was considered. The minimum GDD per day are 5–9 for potato (T_{base} of 2 °C), 10 for soybean (T_{base} of 5 °C) and 9 for sugar beet (T_{base} of 5 °C). Since cold stress does not occur in the major part of the growing cycle, an incorrect estimate of the temperature threshold for transpiration will not strongly affect the simulation of the biomass production.

2.3.1.2. Soil water stress. In FAO56 (Allen et al., 1998) a single soil water depletion factor (p) is used, which is 0.55 for alfalfa hay (Fig. 2). The p factor is the fraction of available soil water that can be depleted from the root zone before transpiration is reduced below its potential. In AquaCrop, following Hsiao (1973), a distinction is made among three soil water stress levels that: (i) reduce canopy expansion, (ii) induce stomatal closure, and (iii) trigger early canopy senescence (Fig. 2). Numerous studies have confirmed that leaf expansion (hence the canopy) is the most sensitive to soil water deficits, and that stomatal conductance and hence transpiration is substantially less sensitive (Steduto et al., 2012). For most calibrated crops in AquaCrop, the upper threshold of soil water depletion for canopy expansion is 0.15–0.20 of TAW. Given that stomatal are substantial less sensitive to soil water depletion than canopy growth, depletion factors of 0.15 (upper) and 0.55 (lower) for canopy expansion and 0.60 for stomatal control were selected for alfalfa (Fig. 2). The considered depletion of 0.70 chosen for senescence is a typical value for the various crops which have been calibrated for AquaCrop.

The shape of the water stress curve determines the magnitude of the effect of the stress on the process between the upper and lower thresholds. In FAO56, a linear decrease of K_s is assumed once the allowed depletion p has been exceeded (Fig. 2). In AquaCrop the shape of the K_s

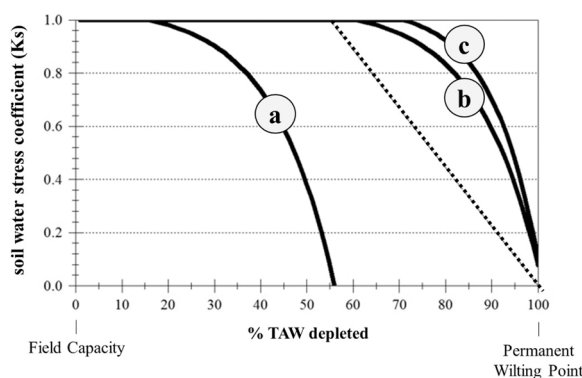


Fig. 2. The AquaCrop soil water stress coefficient (K_s) for various degrees of depletion of the Total Available soil Water (TAW) for (a) canopy expansion, (b) stomatal closure, and (c) senescence, and the single soil water stress coefficient (dotted line) in Allen et al. (1998).

curves is convex which influences the process more strongly when the stress becomes severe, and is more in line with the reduction in matric potential when the soil water content declines. A recent publication (Trout and De Jonge, 2021) supports the hypothesis that a convex K_s curve such as used in AquaCrop, represents better the plant response than a linear function.

2.3.1.3. Soil salinity stress. The upper and lower thresholds for the Electrical Conductivity of soil saturation extract (ECe) are the values given by Ayers and Westcot (1985) for alfalfa. Since salinity stress was not observed in the study sites, the model performance could not be evaluated.

2.3.1.4. Development of Crop Canopy Cover. The average CGC for the calibrated crops in AquaCrop is 0.01 fraction soil cover per growing degree (GD^{-1}) and ranges between 0.004 and 0.020 GD^{-1} . A value of 0.012 GD^{-1} was selected for alfalfa which is slightly above the average to consider the accelerated growth after each cutting. The value allowed the crop to reach full canopy cover between cuttings in absence of stress. Typical values for CDC of calibrated crops in AquaCrop range between 0.003 GD^{-1} and 0.010 GD^{-1} . A value of 0.006 GD^{-1} was selected for alfalfa which is within the range of the CDC of the calibrated crops.

2.3.1.5. Crop transpiration and biomass production. With a basal crop coefficient (K_{cb}) and a soil water evaporation coefficient, crop transpiration (Tr) is separated from soil evaporation (E) in the dual crop coefficient approach of FAO 56. There, the basal crop coefficient (K_{cb}) at mid-season (effective full cover) for alfalfa hay is 1.15 (Allen et al., 1998). AquaCrop separates ET into Tr and E to avoid the confounding effect of the non-productive consumptive use of water (E). The selected crop transpiration coefficient (K_{cTrx}) proposed for alfalfa in AquaCrop was taken as the K_{cb} of FAO56 or 1.15.

In annual crops, AquaCrop simulates a slow decline in canopy photosynthetic capacity following the achievement of full canopy cover (Steduto et al., 2009). As the canopy ages slowly, it undergoes a progressive though small reduction in maximum transpiration and photosynthetic rate. This is simulated by applying an adjustment factor (f_{age}) that decreases the crop transpiration coefficient (K_{cTrx}) by a constant albeit a slight fraction per day (Table 5). Once the canopy reaches its maximum cover (CC_x), natural senescence results in a declining crop coefficient, transpiration, and biomass production in the latter part of the season. However, as alfalfa is harvested multiple times soon after it reaches maximum cover, the ageing effect does not take place, and at each cut it is reset to zero and remains so as long as CC_x is not reached before the next cut.

2.3.1.6. Rooting depth. Alfalfa has a very deep root system among perennial crops. The tap root often reaches a depth of 1.5–2.0 m the first season, 3–3.5 m by the end of the second year, and ultimately it may extend to depths of 6.0 m or more in unrestricted soils (Weaver, 1926; Sun et al., 2008; Undersander et al., 2011). However, in AquaCrop the maximum rooting depth of perennials such as alfalfa is simulated to reach its maximum value near the end of the first season and to remain constant in the successive years after sowing. As indicated in Table 5, the rooting depth increased from 0.3 m (a default AquaCrop value which refers to the depth from which the germinating seedling can extract water) to 3 m deep at the end of the sowing year (as indicated in FAO56 for an open, unrestricted soil). In the successive years after sowing, rooting depth remains at 3 m. Users can adjust the maximum rooting depth in the model according to their own soil conditions.

2.3.1.7. Canopy cover. In AquaCrop canopy cover (CC) is expressed as the fraction or percentage ground cover. The initial canopy cover (CC_0) at germination is determined by the sowing or planting density. It is assumed that an individual seedling at the time of its establishment

covers 2.0 cm² of the soil surface, and that the plant density is 2.5 million plants per hectare (Table 5). These values produce an initial canopy cover (CCo) of 5%. The Canopy Growth Coefficient (expressed as increase of ground cover per growing degree) embedded in a logistic growth function, describes the expansion of CC from CCo to the maximum canopy cover (CCx) in the absence of stress (Steduto et al., 2009). For optimal conditions CCx is determined by crop species and plant density. The considered 95% for alfalfa CCx is the default value in AquaCrop for an ‘almost entirely covered’ situation.

By considering (i) the crop coefficient after cutting ($K_{c_{low}} = 0.3-0.5$; Doorenbos and Pruitt, 1977), (ii) the crop coefficient when canopy is complete ($K_{c_{Tr,x}} = 1.15$; Table 5; Wright, 1988), and (iii) the adjustment in the simulations of the canopy cover (CC*) when CCx is not yet reached (Raes et al., 2022), it was estimated that after each cut, the canopy cover was 25% (CCcut). At the start of a non-planting year, an initial canopy cover of 50% was assumed (Guitjens, 1990).

2.3.1.8. Calibration of WP*. By running simulations with the set of the common parametrized parameters (Table 5), WP* was derived from Eq. 1 by considering the observed dry-biomass and simulated Tr (Table 6). To avoid the confounding effect of possibly incorrectly estimated thresholds for soil water and soil fertility stress, (i) data from Ottawa were excluded and (ii) only data from the 100% irrigation fields in Isparta and from years with limited soil water stress (2014 and 2016) in LLN were considered. Furthermore, by eliminating the data from the 1st cut, the effect of cold stress on Tr and the period of important remobilization of assimilates were eliminated. To avoid the effect of significant storage of assimilates, data of the second half of the season were also excluded. Finally, the derived WP* was normalized by considering the CO₂ concentration (369.41 ppm) for the reference year 2000 (Steduto et al., 2007). Although data dispersion was high due to the remobilization and/or storage of assimilates, an average of 15 g/m² was estimated as the value for WP* (Table 6).

2.3.2. Length of the growing cycle

The selected air temperature criterion for the onset and end of the growing cycle are specified in Table 7. For determining the restart of regrowth in Louvain-La-Neuve and Isparta, air temperature data was appraised in a 120 days’ time window starting at 1 January. For determining the end, the time window was 90 days long, finishing on 31 December. Since the average minimum air temperature in Ottawa is below zero from November till April (Fig. 1.3 in supplementary material), the 120 days’ time window for the onset started at 1 April. For determining the end, the time window was 60 days long and finished on 31 October.

2.3.3. Transfer of assimilates between the above and the below-ground parts

To simulate the transfer of assimilates between the above and the below-ground parts, only three crop parameters are required in

Table 6

Observed dry-biomass (B) and simulated sum of daily crop transpiration (Tr) normalized for climate (ETo) between 2 harvest events, derived WP* from Eq. 1 and after normalisation for CO₂ for the year 2000, for periods where the net transfer of assimilates are likely to be small, and soil water, soil fertility and cold stress are small to negligible.

Site	Period	Cut	B gr/m ²	Σ (Tr/ETo)	derived WP*		Transfer of assimilates
					Eq.1 gr/m ²	Normalized gr/m ²	
LLN	21/5–23/6/2014	2	583	29.9	19.5	18.2	End mobilization
LLN	24/6–22/7/2014	3	340	23.0	14.8	13.8	Start storage
LLN	20/5–6/7/2016	2	519	47.2	11.0	10.2	Start storage
Isparta	11/5–11/6/2018	2	748	30.6	24.4	22.3	End mobilization
Isparta	12/7–21/7/2018	3	496	39.0	12.7	11.6	Start storage
Isparta	18/5–24/6/2019	2	677	38.8	17.5	15.8	End mobilization
Isparta	25/6–29/7/2019	3	424	36.3	11.7	10.6	Start storage
Average						15	

Table 7

Air temperature criterion for generating the onset and end of the growing cycle.

Period	Sum GDD	Period	Occurrence
Onset	≥ 20	8 days	2nd
End	≤ 10	8 days	2nd

AquaCrop: (i) the start of the net storage stage, (ii) the remobilization (M) and (iii) the storage (S) fractions (Fig. 1). These parameters are mainly cultivar specific and can be calibrated with observed yield data. However, to illustrate the robustness of the simulation process, a fine-tuning for each of the study sites was not attempted. For all 3 cultivars the following assumptions were made:

- storage started at mid-June to mid-July, which is 180 days before the end of the growing cycle for Louvain-La-Neuve and Isparta, and 100 days for Ottawa where alfalfa has a shorter growing cycle;
- 60% of the stored assimilates were remobilized in the next season ($M = 0.60$).

Given that high latitude cultivars have more seasonality with higher biomass partitioning below ground in late summer/autumn in response to lower temperatures and shorter daylength (Moot et al., 2012), the storage fraction (S) at the end of the growing cycle, was chosen as 0.65 for Louvain-La-Neuve and Ottawa, and 0.45 for Isparta. The S values also reflected the differences among alfalfa cultivars, according to their Mediterranean or northern origin.

2.3.4. Soil fertility stress

In Ottawa, no N fertilizer was applied (Jing et al., 2020). By running simulations without soil fertility stress, the maximum attainable total biomass production (Bmax) in the 3 years of observations was about double of the observed yields (reported measurements were 47%, 55%, and 46% of simulated Bmax in the three successive years). In AquaCrop, soil fertility stress is evaluated through Brel, which is the relative biomass production with reference to Bmax, that can be achieved for a given soil fertility level in the absence of water or any other stress (Van Gaelen et al., 2014). By calibrating alfalfa with a Brel of 50%, AquaCrop selects values for the three fertility stress coefficients affecting canopy development (CC) and the single coefficient affecting WP*, to achieve the specified Brel. The target crop parameters for the three coefficients affecting CC are respectively CGC, CCx and a decline of CC after mid-season. In absence of field data allowing a fine-tuning of the individual stress coefficients, the default setting for the 4 stress coefficients was considered. The default values corresponded to a 40% and 20% reduction respectively for CCx and CGC, a 0.04%/day decline of CC, and a stress coefficient which gradually reduced WP* from 15 g/m² at the start of the season to 7.2 g/m² at the end of the season when the nutrient reservoir became depleted.

2.4. Simulation runs

All simulations were run with the common set of parameterized crop parameters (Table 5). Simulations started in the sowing year for Ottawa and LLN. Due to the absence of data for the sowing year for Isparta, the first simulation was one year after sowing.

Since the soil water content at the time of sowing was unknown, simulations started with bare soil on 1 January well before sowing in Louvain-La-Neuve and Ottawa. Given the importance of winter rains relative to the small to negligible ETo, it was assumed that the soil profile was at Field Capacity (FC) on that day. By keeping track of the rainfall, soil evaporation and deep percolation on the successive days of the simulation period, AquaCrop obtained the soil water content at the specified day of sowing. For Isparta, simulations started on 1 January of the 1st year after sowing. Given the high ETo and relative low rainfall during the year (Table 2), only the top 0.60 m of the soil profile was assumed to be at FC and the rest of the profile at 50% of TAW at the start of the simulations.

Apart from the sowing years, simulations were run for the 2 (Ottawa and Isparta) and 3 (LLN) years after sowing and for the 5 different irrigation strategies in Isparta. Each simulation run stopped at the generated end of the growing cycle for the considered year (Fig. 3). The run for the next year, started on the day after the generated end of the growing cycle of the previous year. The initial soil water content at the start of a run was given by the soil water content at the end of the previous run.

To evaluate the simulated above-ground biomass (dry matter) four statistical indicators were used (the equations are presented in Chapter 4 of the supplementary material): the coefficient of correlation (r^2), the Normalized Root Mean Square Error (nRMSE), the Nash-Sutcliffe model efficiency coefficient (EF), and the Willmott's index of agreement (d).

3. Results and discussion

The generated onsets, ends and lengths of the growing cycle for alfalfa for each of the study sites and simulated years are presented in Table 8.

The cold stress affecting crop transpiration (and hence biomass production) at the start and end of the growing cycle, led to low biomass production at the start and end of the generated growing period, where the growing degrees were generally smaller than the minimum required for full crop transpiration (assessed at 8 °C – day in Table 5). This greatly reduced the effects of possible errors in the start and end of the growing cycle. For a representative simulation of the generated growing cycle (Fig. 4), the relative biomass production (Eq. 1) was only 5% of the total production in the first 30 days and 3% in the last 30 days of the cycle. The simulations results would have been hardly affected if the noted start and end of the cycle was in fact later or earlier.

The simulated and observed cumulative biomass, increasing at each harvest, for the three study sites, irrigation strategy, and for all years are presented in Fig. 5. Since cumulative biomass can compensate an over (under) yield estimate at one harvest by a similar under (over) yield

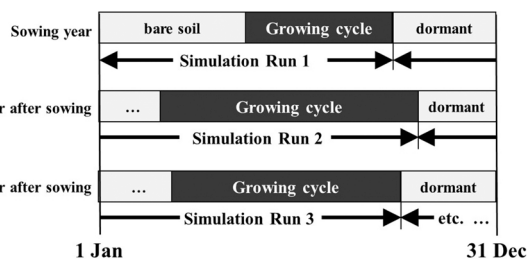


Fig. 3. Schematic presentation of the linked simulation runs starting (i) on 1 January for the sowing year and (ii) on the day after the generated end of the growing cycle of the previous years for the successive years after sowing.

Table 8

Generated onset, end, and length of the growing cycle.

Site	Year after sowing	Onset	End	Length (days)
Louvain-La-Neuve	Sowing year	8 May 2013	10 Dec 2013	217
	1st	27 Feb 2014	10 Dec 2014	287
	2nd	15 Apr 2015	27 Nov 2015	227
Isparta	3rd	9 Feb 2016	1 Dec 2016	297
	1st	17 March 2018	12 Dec 2018	271
Ottawa	2nd	8 April 2019	16 Dec 2019	253
	Sowing year	21 May 2014	31 Oct 2014	164
	1st	1 May 2015	24 Oct 2015	177
	2nd	7 May 2016	28 Oct 2016	175

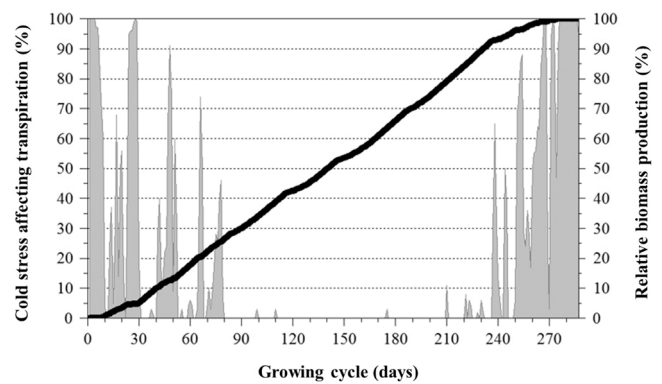


Fig. 4. Simulated cold stress affecting crop transpiration of alfalfa (bars) and corresponding relative biomass production (line) in Louvain-La-Neuve in 2014 between the generated onset (27 February) and end (10 December) of the growing cycle.

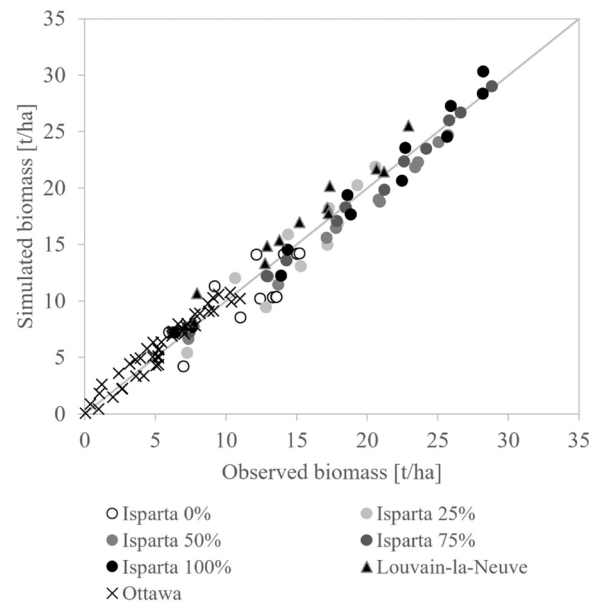


Fig. 5. Observed and simulated cumulative dry above ground biomass, increasing at each harvest, for alfalfa for all years and irrigation strategies for Louvain-La-Neuve (triangles), Isparta (circles), and Ottawa (crosses).

estimate at the next harvest, also the individual simulations for all the 81 harvest events were evaluated (Fig. 6). The statistical evaluation is given in Table 9.

The statistical evaluation (Table 9) indicates that AquaCrop simulated well the observed yield in the three different environments with a common set of parametrized crop parameters and a tentatively calibrated WP*. The evaluation of the cumulative dry above-ground biomass (Fig. 5) indicates that the simulated results are good to very good. The indicators r^2 , nRMSE and EF indicate a (very) small dispersion between observed and simulated biomass. The evaluation of the 81 individual harvests (Fig. 6) still confirms the quality of the model, although the nRMSE (moderate good) shows that the dispersion is twice as large then for the cumulative biomass. The high value of the d indicator confirms that there is no systematic over- or underestimation by the model.

Aquacrop differs from other crop simulation models by its water-driven growth-engine, in which the daily biomass production (b_t) is made proportional to the amount of water consumed as crop transpiration (Eq. 1) through a normalized water productivity parameter (WP*). In other alfalfa models, which are carbon or solar driven, growth is based on carbon assimilation by the photosynthesis, and the key parameter relating biomass to intercepted radiation is the radiation use efficiency (RUE). To complete the simulation of biomass production, other models also consider the maintenance and growth respiration of the various organs and the partition of the structural biomass amongst the various plant organs (stem, leaves, roots and storage organs). Although such calculation scheme is more explanatory than that of AquaCrop, RUE models require knowledge of an extended number of variables and input parameters which are not easily available, and much more familiar to scientists than to end users. In contrast, Aquacrop requires only three extra crop parameters (see Section 2.3.3) to simulate the transfer of assimilates between the above and the below-ground parts in alfalfa. Additionally, the transfer of assimilates can be easily calibrated by altering (i) the storage fraction (S) at the end of the growing cycle, and/or (ii) the remobilization fraction (M) in the next season and/or (iii) the storage time. Notwithstanding the huge simplification of the transfer processes subroutine, the results suggest that AquaCrop performs as well or even better than other, more complex models in the simulation of alfalfa yield (Table 10).

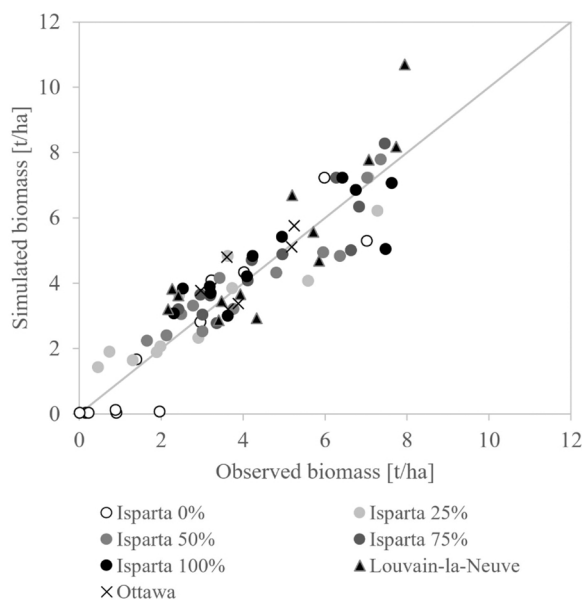


Fig. 6. Observed and simulated dry-biomass yield of alfalfa for each of the 81 individual harvest events for Louvain-La-Neuve (triangles), Isparta (circles), and Ottawa (crosses).

Table 9

Evaluation of the simulated (i) cumulative above-ground biomass (Fig. 5) and (ii) the biomass for each of the 81 individual harvest events (Fig. 6), by the coefficient of correlation (r^2), the normalized Root Mean Square Error (nRMSE), the Nash-Sutcliffe model efficiency coefficient (EF), and the Willmott's index of agreement (d).

Indicator	Cumulative biomass (Fig. 5)		Biomass of Individual harvest events (Fig. 6)	
	Value	Evaluation	Value	Evaluation
r^2	0.97	Very good (≥ 0.90)	0.83	Good (0.80 – 0.89)
nRMSE	11%	Good (6 – 15%)	22%	Moderate good (16 – 25%)
EF	0.97	Very good (≥ 0.80)	0.81	Very good (≥ 0.80)
d	0.99	Very good (≥ 0.90)	0.95	Very good (≥ 0.90)

The simulated green canopy cover, the remobilized and stored assimilates, and the observed and simulated cumulative above-ground biomass during the growing cycle of alfalfa for all years, irrigation managements and study sites are presented in Chapter 5 of the supplementary material. As an example, the simulation results for the 2nd year after sowing for Isparta for the 75% ET irrigated treatment are presented in Fig. 7. As can be observed in the central plot, the simulated transfer of assimilates differed from the theoretical functions (Fig. 7: dotted lines), because the transfer was affected by: (i) cold stress, which was severe at the start and end of the season; (ii) the frequency of cuttings; and (iii) soil water deficits. The response of the transfer to stresses and frequency of cuttings allows AquaCrop to simulate the negative effect of water stress and/or late cuttings on the amount of stored assimilates at the end of the season. When the root reserves are too low during the winter period, insufficient carbohydrates can be remobilized at the start of the next season to accelerate regrowth.

Fine tuning of the water stress parameters was not possible as sufficient field data was not available. Nevertheless, with the parametrized set (Table 5), the effect of water stress on alfalfa yield was well simulated in the water stressed treatments. For the 2nd year after sowing for LLN, and the 75%, 50% and 25% ET irrigated treatments in Isparta, the nRMSE remained below 15% (good). Only for the rainfed alfalfa in Isparta, resulting in very severe water stress, the nRMSE increased to 25% (moderate good) and this only for the 2nd year after sowing. This moderately good result might be partly linked to the fixed rooting depth (at 3 m) considered by AquaCrop for all the years after sowing. Since it has been reported in the literature that the taproot still expands in the following years and it may ultimately reach a depth of 6.0 m or more in unrestricted soils (Weaver, 1926; Sun et al., 2008; Undersander et al., 2011), it is possible that rainfed alfalfa could have drawn stored water from the winter rains from the soil layers below 3 m. The restricted rooting depth in AquaCrop to 3 m may therefore be the cause for the underprediction of biomass production at the beginning of the 2nd year of rainfed alfalfa (Fig. 5.2 h and 5.2j in the Supplementary Materials).

With the common air temperature criterion for generating the onset and end of the growing cycle, together with the estimated cold threshold for transpiration, good to very good estimates of alfalfa yield were obtained, notwithstanding that the criterion and thresholds might differ for other cultivars and climatic conditions.

In AquaCrop WP* for C3 crops ranges between 15 and 20 g/m². The simulation results indicated that with a WP* of 15 g/m² for alfalfa, very good estimates of yields were obtained. However, the value should be regarded as a first conservative estimate for alfalfa as it is not known with certainty that soil fertility was optimal in all sites used in this calibration. If soil fertility was limiting yields, then one would expect the value of WP* to be above 15 g/m².

4. Conclusions

An extension of the AquaCrop model to simulate a perennial crop, alfalfa, is presented here. The processes of assimilate storage below ground and the subsequent remobilization to supplement above ground

Table 10

Evaluation of the simulations of alfalfa biomass using other crop models, with indication of the coefficient of correlation (r^2), the normalized Root Mean Square Error (nRMSE), the Nash-Sutcliffe model efficiency coefficient (EF), and the Willmott's index of agreement (d).

Crop model	Application	Statistical indicator				Reference
		r^2	nRMSE	EF	d	
CSM-CROPGRO -PFM	Northern Spain,	-	26%	-	0.75	Malik et al. (2018)
	Eastern Canada	-	24%	-	0.86	
APSIM-Lucerne	a) Argentine Pampas, and S-E Australia:					Ojeda et al. (2016)
	Alfalfa biomass	0.59	-	0.53	-	
	Total annual yields	0.87	-	0.86	-	
	b) China:					Peng et al. (2022)
Alfalfa biomass	0.40	27%	-	-		
Total annual yields	0.81	13%	-	-		
STICS	France: biomass regrowth	0.69	35%	0.65	-	Brisson et al. (1998)

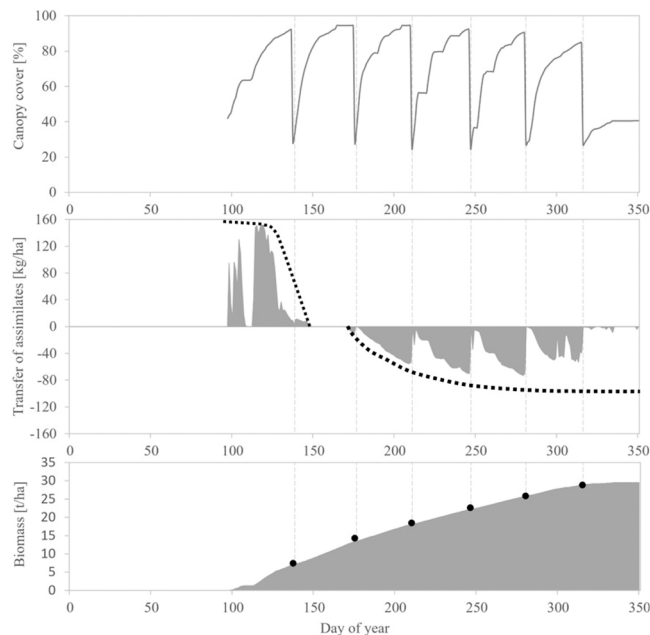


Fig. 7. Simulated green canopy cover (top), the simulated (grey area) transfer of assimilates (remobilization (positive) and storage (negative)) with indication (dotted line) of the theoretical (Fig. 1) remobilization (Eq. 6) and storage (Eq. 3) function, and the observed (dots) and simulated (grey area) cumulative dry above-ground biomass (bottom) during the growing cycle (8 April – 16 December 2019) of alfalfa, for the 2nd year after sowing for the 75% ET irrigated treatment in Isparta. Day 1 is 1 January and nRMSE is 1.9%.

growth were simulated in a simple way by multiplying the biomass water productivity (WP^*) with a correction factor greater than one during the remobilization stage, and smaller than one during the storage stage. Experimental data from three different environments vastly different in climate such as Canada, Belgium, and Turkey were used to calibrate the model. The comparisons between measurements and the simulations indicated that AquaCrop can well predict the total yield of alfalfa that can be expected in various climates and environments, with and without water stress and soil fertility stress, for three different alfalfa cultivars.

Declaration of Competing Interest

The authors declare that they have no known competing financial interests or personal relationships that could have appeared to influence the work reported in this paper.

Data Availability

The authors do not have permission to share data.

Acknowledgment

The Isparta research was supported by TUBITAK project 2150326 (Y. Ucar, M.Turk, and S.Kale Celik).

Appendix A. Supporting information

Supplementary data associated with this article can be found in the online version at doi:10.1016/j.agwat.2023.108341.

References

- Allen R., Pereira, L., Raes, D., and Smith, M. 1998. Crop Evapotranspiration - Guidelines for computing crop water requirements. FAO Irrigation and Drainage paper N° 56. Rome, Italy. Website: <http://www.fao.org/docrep/X0490E/X0490E00.htm>.
- Araya, A., Kisekka, I., Holman, J., 2016. Evaluating deficit irrigation management strategies for grain sorghum using AquaCrop. *Irrig. Sci.* 34, 465–481.
- Asseng, S., Hsiao, T.C., 2000. Canopy CO₂ assimilation, energy balance, and water use efficiency of an alfalfa crop before and after cutting. *Field Crops Res.* 67 (3), 191–206.
- Avice, J.C., Ourry, A., Boucaud, J., 1996. Nitrogen and carbon flows estimated by 15N and 13C pulse-chase labeling during regrowth of alfalfa. *Plant Physiol.* 112, 281–290. <https://doi.org/10.1104/pp.112.1.281>.
- Ayers, R.S. and D.W. Westcot. 1985. Water quality for agriculture. FAO Irrigation and Drainage Paper N° 29. Rome, Italy. 174 p.
- Baral, R., Lollato, R.P., Bhandari, K., Min, D., 2022. Yield gap analysis of rainfed alfalfa in the United States. *Front. Plant Sci.* (13) <https://doi.org/10.3389/fpls.2022.931403>.
- Brisson, N., Mary, B., Ripoche, D., Jeuffroy, M.H., Ruget, F., Nicoullaud, B., Gate, P., Devienne-Barret, F., Antonioletti, R., Duru, C., 1998. STICS: a generic model for the simulation of crops and their water and nitrogen balances. I. Theory and parameterization applied to wheat and corn. *Agronomie* 18, 311–346.
- Confalonieri, R., Bechini, L., 2004. A preliminary evaluation of the simulation model CropSyst for alfalfa. *Eur. J. Agron.* 21, 223–237.
- Di Paola, A., Valentini, R., Santini, M., 2015. An overview of available crop growth and yield models for studies and assessments in agriculture. *J. Sci. Food Agric.* 96 (3) <https://doi.org/10.1002/jsfa.7359>.
- Doorenbos, J., Pruitt, W.O., 1977. Guidelines for Predicting Crop Water Requirements. FAO Irrigation and Drainage, Rome, Italy.
- FAOSTAT, 2022. FAOSTAT Database. FAO, Rome, Italy. <http://faostat.fao.org/> (accessed 23 December 2022).
- Farahani, H.J., Izzi, G., Oweis, T.Y., 2009. Parameterization and evaluation of the AquaCrop model for full and deficit irrigated cotton. *Agron. J.* 101 (3), 469–476.
- García-Vila, M., Morillo-Velarde, R., Fereres, E., 2019. Modeling sugar beet responses to irrigation with AquaCrop for optimizing water allocation. *Water* 11, 1918. <https://doi.org/10.3390/w11091918>.
- García-Vila, M., Fereres, E., Mateos, L., Orgaz, F., Steduto, P., 2009. Deficit irrigation optimization of cotton with AquaCrop. *Agron. J.* 101 (3), 477–487.
- Geerts, S., Raes, D., García, M., Miranda, R., Cusicanqui, J.A., Taboada, C., Mendoza, J., Huanca, R., Mamani, A., Condori, O., Mamani, J., Morales, B., Osco, V., Steduto, P., 2009. Simulating yield response of quinoa to water availability with AquaCrop. *Agron. J.* 101 (3), 499–508.
- Guilpart, N., Grassini, P., Sadras, V.O., Timsina, J., Cassman, K.G., 2017. Estimating yield gaps at the cropping system level. *Field Crops Res.* 206, 21–32. <https://doi.org/10.1016/j.fcr.2017.02.008>.
- Guitjens, J.C. 1990. Alfalfa In: Irrigation of Agricultural Crops, B.R.Stewart and D. R. Nielsen, (eds). Amer. Soc. Agron. Mon. # 30, Madison, Wis. USA: 535–568.

- Heng, L.K., Hsiao, T.C., Evett, S., Howell, T., Steduto, P., 2009. Validating the FAO AquaCrop model for irrigated and water deficient field maize. *Agron. J.* 101 (3), 488–498.
- Hoogenboom, G., Porter, C.H., Boote, K.J., Shelja, V., Wilkens, P.W., Singh, U., White, J. W., Asseng, S., Lizaso, J.I., Moreno, L.P., Pavan, W., Ogoshi, R., Hunt, L.A., Tsuji, G. Y., Jones, J.W., 2019. The DSSAT crop modeling ecosystem. In: p.173–216. In: Boote, K.J. (Ed.), *Advances in Crop Modeling for a Sustainable Agriculture*. Burleigh Dodds Science Publishing, Cambridge, United Kingdom. <https://doi.org/10.19103/AS.2019.0061.10>.
- Hsiao, T.C., 1973. Plant responses to water stress. *Annu. Rev. Plant Physiol.* 24, 519–570. <https://doi.org/10.1146/annurev.pp.24.060173.002511>.
- Hsiao, T.C., Heng, L., Steduto, P., Rojas-Lara, B., Raes, D., Fereres, E., 2009. III. Parameterization and testing for maize. *Agron. J.* 101 (3), 448–459.
- Jing, Q., Qian, B., Bélanger, G., VanderZaag, A., Jégo, G., Smith, W., Grant, B., Shang, Liu, J., He, W., Boote, K., Hoogenboom, G., 2020. Simulating alfalfa regrowth and biomass in eastern Canada using the CSM-CROPGRO-perennial forage model. *Eur. J. Agron.* 113. <https://doi.org/10.1016/j.eja.2019.125971>.
- Keating, B.A., Carberry, P.S., Hammer, G.L., Probert, M.E., Robertson, M.J., Holzworth, D., Huth, N.I., Hargreaves, J.N.G., Meinke, H., Hochman, Z., McLean, G., Verburg, K., Snow, V., Dimes, J.P., Silburn, M., Wang, E., Brown, S., Bristow, K.L., Asseng, S., Chapman, S., McCown, R.L., Freebairn, D.M., Smith, C.J., 2003. An overview of APSIM, a model designed for farming systems simulation. *Eur. J. Agron.* 18, 267–288. [https://doi.org/10.1016/S1161-0301\(02\)00108-9](https://doi.org/10.1016/S1161-0301(02)00108-9).
- Kumar, P., Sarangi, A., Singh, D.K., Parihar, S.S., 2014. Evaluation of AquaCrop model in predicting wheat yield and water productivity under irrigated saline regimes. *Irrig. Drain.* 63, 474–487.
- Loomis, R.S., Connor, D.J., 2012. *Crop Ecology: Productivity and Management in Agricultural Systems*. Cambridge University Press, UK. <https://doi.org/10.1017/CBO9781139170161>.
- Malik, W., Boote, K.J., Hoogenboom, G., Cavero, J., Dechmi, F., 2018. Adapting the CROPGRO model to simulate alfalfa growth and yield. *Biometry, Model. Stat.* 110 (5), 1–14. <https://doi.org/10.2134/agronj2017.12.0680>.
- Moot, D., Teixeira, E., Brown, H. 2012. Alfalfa. In Steduto et al. (Ed). Crop yield response to water. *FAO Irrigation and Drainage Paper* Nr. 66. Rome, Italy: 212–219. <https://researcharchive.lincoln.ac.nz/bitstream/handle/10182/6262/MootAlfalfachapter.pdf;sequence=1>.
- Moot, D.J., Brown, H.E., Teixeira, E.I., and Pollock, K.M. 2003. Crop growth and development affect seasonal priorities for lucerne management. In "Legumes for dryland pastures" (D. J. Moot, ed.): 201–208. New Zealand Grassland Association, Lincoln, Canterbury, New Zealand.
- Ojeda, J.J., Pembleton, K.G., Islam, M.R., Agnusevi, M.G., Garcia, S.C., 2016. Evaluation of the agricultural production systems simulator simulating Lucerne and annual ryegrass dry matter yield in the Argentine Pampas and south-eastern Australia. *Agric. Syst.* 143, 61–75. <https://doi.org/10.1016/j.agry.2015.12.005>.
- Orloff, S.B., Putnam, D.H., 2007. Harvest strategies for alfalfa. In "Irrigated alfalfa management for Mediterranean and Desert zones". Chapter 13. Univ. Calif. Agric. Nat. Resour. Publ. 8299. <http://alfalfa.ucdavis.edu/IrrigatedAlfalfa>.
- Peng, Y., Li, Z., Sun, T., Zhang, F., Wu, Q., Du, M., Sheng, T., 2022. Modeling long-term water use and economic returns to optimize alfalfa-corn rotation in the corn belt of northeast China. *Field Crops Res.* 276. <https://doi.org/10.1016/j.fcr.2021.108379>.
- Raes, D., Steduto, P., Hsiao, T.C., Fereres, E., 2009. II Main algorithms and software description. *Agron. J.* 101 (3), 438–447.
- Raes, D., Steduto, P., Hsiao, T.C., Fereres, E., 2022. AquaCrop Reference manual. Version 7.0. FAO, Rome, Italy. <http://www.fao.org/nr/water/aquacrop.html>.
- Razzaghi, F., Zhou, Z., Andersen, M.N., Plauborg, F., 2017. Simulation of potato yield in temperate condition by the AquaCrop model. *Agric. Water Manag.* 191, 113–123.
- Salman, M., Garcia-Vila, M., Fereres, E., Raes, D., Steduto, P., 2021. The AquaCrop Model: Enhancing Crop Water Productivity. *FAO Water reports* 47, Rome, Italy.
- Steduto, P., Hsiao, T.C., Fereres, E., 2007. On the conservative behavior of biomass water productivity. *Irrig. Sci.* 25, 189–207.
- Steduto, P., Hsiao, T.C., Raes, D., Fereres, E., 2009. I. Concepts and underlying principles. *Agron. J.* 101 (3), 426–437.
- Steduto, P., Hsiao, T.C., Fereres, E., Raes, D., 2012. Crop Yield Response to Water. *FAO Irrigation and Drainage*, Rome, Italy. <http://www.fao.org/nr/water/aquacrop.html>.
- Strullu, L., Beaudoin, N., Thiébau, P., Julier, B., Mary, B., Ruget, F., Ripoche, D., Rakotovololona, L., Louarn, G., 2020. Simulation using the STICS model of C&N dynamics in alfalfa from sowing to crop destruction. *Eur. J. Agron.* 112, 125948. <https://doi.org/10.1016/j.eja.2019.125948>.
- Sun, H.R., Wu, R.X., Li, P.H., Shao, S., Qi, L.L., Han, J.G., 2008. Rooting depth of alfalfa. *Acta Agrestia Sin.* 16 (3), 307.
- Teixeira, E.I., Moot, D.J., Brown, H.E., 2008. Defoliation frequency and season affected radiation use efficiency and dry matter partitioning to roots of lucerne (*Medicago sativa*, L.) crops. *Eur. J. Agron.* 28 (2), 103–111.
- Todorovic, M., Albrizio, R., Zivotic, L., Abi Saab, M.T., Stöckle, C., Steduto, P., 2009. Assessment of AquaCrop, CropSyst, and WOFOST models in the simulation of sunflower growth under different water regimes. *Agron. J.* 101 (3), 509–521.
- Trout, T.J., De Jonge, K.C., 2021. Evapotranspiration and water stress coefficient for deficit-irrigated maize. *J. Irrig. Drain. Eng.* 147 (10) [https://doi.org/10.1061/\(ASCE\)IR.1943-4774.0001600](https://doi.org/10.1061/(ASCE)IR.1943-4774.0001600).
- Tsegay, A., Vanuytrecht, E., Abrha, B., Deckers, J., Gebrehiwot, K., Raes, D., 2015. Sowing and irrigation strategies for improving rainfed tef (*Eragrostis tef* (Zucc.) Trotter) production in the water scarce Tigray region, Ethiopia. *Agric. Water Manag.* 150, 81–91.
- Undersander, D., Cosgrove, D., Cullen, E., Grau, C., Rice, M.E., Renz, M., Sheaffer, C., Shewmaker, G., Sulc, M. 2011. Alfalfa management guide. American Society of Agronomy, Inc. Crop Science Society of America, Inc. Soil Science Society of America, Inc., Madison (WI), USA. <https://www.agronomy.org/files/publications/alfalfa-management-guide.pdf>.
- Van Gaelen, H., Tsegay, A., Delbecq, N., Shrestha, N., Garcia, M., Fajardo, H., Miranda, R., Vanuytrecht, E., Abrha, B., Diels, J., Raes, D., 2014. A semi-quantitative approach for modelling crop response to soil fertility: evaluating of the AquaCrop procedure. *J. Agric. Sci.* 153, 1218–1233.
- Van Gaelen, H., Delbecq, N., Abrha, B., Tsegay, A., Raes, D., 2016. Simulation of crop water productivity in weed-infested fields for data-scarce regions. *J. Agric. Sci.* 154 (6), 1026–1039.
- van Keulen, H., Asseng, S., 2019. Simulation Models as Tools for Crop Management. In: Savin, R., Slafer, G. (Eds.), *Crop Science. Encyclopedia of Sustainability Science and Technology Series*. Springer, New York, NY. https://doi.org/10.1007/978-1-4939-8621-7_1047.
- Vanuytrecht, E., Raes, D., Steduto, P., Hsiao, T.C., Fereres, E., Heng, L.K., Garcia Villa, M., Mejias Moreno, P., 2014. AquaCrop: FAO's crop water productivity and yield response model. *Environ. Model. Softw.* 62, 351–360.
- Weaver, J.E. 1926. Root habits of alfalfa (Chapter XIII in Root development of field crops). McGraw-Hill Book Company, Inc., New York, USA. <https://soilandhealth.org/wp-content/uploads/01aglibrary/010139fieldcroproots/010139toc.html>.
- Wellens, J., Raes, D., Traore, F., Denis, A., Djaby, B., Tychon, B., 2013. Performance assessment of the FAO AquaCrop model for irrigated cabbage on farmer plots in a semi-arid environment. *Agric. Water Manag.* 127, 40–47.
- Wright, J.L., 1988. Daily and seasonal evapotranspiration and yield of irrigated alfalfa in southern Idaho. *Agron. J.* 80 (4), 662–669.
- Yuegao, H. and Cash, D. 2009. Global status and development trends of alfalfa. In: *Alfalfa management guide for Ningxia*; Ed. Cash, D; United Nations Food and Agricultural Organization. 114 p.